ANTIOXIDANTS & REDOX SIGNALING
Volume 13, Number 8, 2010

DOI: 10.1089/ars.2010.3119

FORUM REVIEW ARTICLE

The PAPS-Independent Aryl Sulfotransferase and the Alternative Disulfide Bond Formation System in Pathogenic Bacteria

Goran Malojčić and Rudi Glockshuber

Abstract

Sulfurylation of biomolecules (often termed sulfonation or sulfation) has been described in many organisms in all kingdoms of life. To date, most studies on sulfotransferases, the enzymes catalyzing sulfurylation, have focused on 3′-phosphate-5′-phosphosulfate (PAPS)-dependent enzymes, which transfer the sulfuryl group from this activated anhydride to hydroxyl groups of acceptor molecules. By contrast, the PAPS-independent aryl sulfotransferases (ASSTs) from bacteria, which catalyze sulfotransfer from phenolic sulfate esters to another phenol in the bacterial periplasm, were not well characterized until recently, although they were first described in 1986 in a search for nonhepatic sulfurylation processes. Recent studies revealed that this unusual class of sulfotransferases differs profoundly in both molecular structure and catalytic mechanism from PAPS-dependent sulfotransferases, and that ASSTs from certain bacterial pathogens are upregulated during infection. In this review, we summarize the literature on the roles of sulfurylation in prokaryotes and analyze the occurrence of ASSTs and their dependence on Dsb proteins catalyzing oxidative folding in the periplasm. Furthermore, we discuss structural differences and similarities between aryl sulfotransferases and PAPS-dependent sulfotransferases. *Antioxid. Redox Signal.* 13, 1247–1259.

Introduction: Sulfurylation and Sulfotransferases

The sulfurylation of biologic molecules has been described in all kingdoms of life, and a variety of small biomolecules, including hormones, sugars, and antibiotics, have been identified as sulfurylation substrates. Together with glucuronidation, sulfurylation is well known to increase the water solubility of endogenous and exogenous phenolic compounds and forms a major detoxification route in the liver. In addition, sulfurylated molecules regulate communication outside the cell and are known to mediate interactions between eukaryotic hosts and prokaryotic pathogens during infection (see later) (18, 19, 30).

Sulfotransferases catalyze the transfer of a sulfuryl group from a donor to an acceptor substrate. Based on their specificity toward the donor, sulfotransferases can be classified into adenosine 3′-phosphate-5′-phosphosulfate (PAPS)-dependent or PAPS-independent enzymes. Whereas PAPS-dependent sulfotransferases, which are present in the bacterial or eukaryotic cytosol or the Golgi apparatus in eukaryotes, have been very extensively studied [for recent reviews, see (6, 10)], this review focuses on the much less characterized class of prokaryotic aryl sulfotransferases (ASSTs), which catalyze the transfer of a sulfuryl group from phenolic sulfate esters onto a phenol in a PAPS-independent manner (Fig. 1) (43). ASSTs are most often found in the periplasm of strains of δ- and ε-proteobacteria, and the corresponding genes are usually clustered on the same operon with genes encoding homologues of DsbA and DsbB, which catalyze disulfide bond formation in the periplasm. Notably, of all *Escherichia coli* (*E. coli*) strains, only the uropathogenic strains contain a gene for ASST. It was found that ASST is upregulated in the uropathogenic habitat, suggesting that ASST might play a role in urinary tract infections (51). The first x-ray structure of an ASST that has been elucidated recently revealed that ASSTs differ substantially from all previously characterized sulfotransferases in their three-dimensional structure and active-site architecture (54).

We review the current knowledge and the open questions related to PAPS-independent aryl sulfotransferases, their occurrence, genomic context, possible biologic roles, molecular structure, and biochemistry.

Sulfurylation in Prokaryotes

As opposed to the large number of catalyzed sulfurylation processes in mammalian cells that have been characterized, relatively few sulfotransferases from prokaryotes have been

Institute of Molecular Biology and Biophysics, ETH Zurich, Zurich, Switzerland.

studied. For example, in the symbiotic relation between the nitrogen-fixing rhizobia and legumes, sulfotransferases play a crucial role in the biogenesis of secreted root-nodulation factors, like the factor Nod from *Sinorhizobium meliloti*. These nodulation factors are signaling molecules between plants and bacteria, critical for the determination of host specificity (19). Another instance of prokaryotic sulfurylation is the production of sulfurylated metabolites in mycobacteria, including the human pathogen *Mycobacterium tuberculosis*. As an example, the biosynthesis of sulfolipid-1 (implicated in *M. tuberculosis* virulence) involves the sulfurylation of its core building block trehalose (59, 60).

Although the sulfurylation of these biomolecules is catalyzed by PAPS-dependent sulfotransferases with defined acceptor-substrate specificities, PAPS-independent sulfurylation by periplasmic ASSTs can be found in commensal intestinal bacteria, where these enzymes accept a variety of aromatic sulfuric acid esters and phenols as sulfuryl donors and acceptors, respectively. For example, ASST from *Eubacterium* A-44, an anaerobic bacterium from human intestine, was reported to sulfurylate phenolic antibiotics, such as amoxicillin, cefadroxil, and cefoperazone (42), and to transfer sulfuryl groups from the laxative sodium picosulfate onto other phenols (36). Furthermore, this enzyme is capable of transferring sulfuryl groups from 4-acetylphenylsulfate, 4-methylumbelliferylsulfate, and 4-nitrophenylsulfate to naphthol, estradiol, phenol, tyrosine methyl ester, tyramine, and epinephrine (Fig. 2), and a variety of other naturally occurring compounds (44). In addition, ASST-catalyzed sulfotransfer between various small phenolic compounds with up to three fused aromatic rings was identified in the rat intestinal bacterium *Klebsiella* K-36 (1, 38). Furthermore, besides glucuronidation, sulfurylation represents a major detoxification pathway in the liver and is suggested to contribute to the detoxification of phenolic compounds (40, 41).

Another example of sulfurylation is found in the gram-negative opportunistic pathogen *Edwardsiella tarda*, where ASST is proposed to be involved in the production of siderophores, small molecules capable of scavenging the essential trivalent iron ions (Fe^{3+}) from the growth medium (57). Further ASSTs also were described in *Citrobacter freundii* (33), *Enterobacter amnigenus* AR-37 (45), *Salmonella typhimurium* (34), *Haemophilus* K-12 (48), as well as in uropathogenic *E. coli* CFT073 (54). That the majority of the natural ASST substrates and the physiologic roles of ASSTs still remain unknown may result from the fact that these enzymes exhibit a rather broad sulfuryl donor and acceptor substrate specificity. In this context, it has been proposed that the main *in vivo* role of ASSTs may be simply to shuffle the sulfuryl group around within a set of phenolic compounds (54). It remains to be established whether a certain subset of preferred sulfuryl donors and a different subset of preferred acceptors exist.

Disulfide Bond-Formation Systems in Bacteria and the Genomic Context of ASST

Structural disulfide bonds are a typical feature of secretory proteins and are often required for protein folding and stability. Formation of a disulfide bond between two cysteines in a newly synthesized protein is a catalyzed redox reaction that requires the interaction of the folding protein with an oxidant that accepts the two electrons generated. In gram-negative bacteria, structural disulfide bonds are formed in the oxidizing environment of the periplasm. The **di**sulfide **b**ond formation (Dsb) proteins catalyze the formation and isomerization of disulfide bonds in bacteria. The periplasmic dithiol oxidase DsbA is a soluble protein with an extremely oxidizing redox potential of −121 mV, which rapidly introduces disulfides into folding proteins (53, 56, 76). *In vivo*, DsbA oxidizes peptides as they are being transferred across the inner membrane into the periplasmic space. Therefore, if a substrate protein contains consecutive disulfide bonds in its native state, DsbA is sufficient for the correct disulfide formation (14), whereas proteins with nonconsecutive disulfides are dependent on DsbC, the *E. coli* catalyst of disulfide reduction and isomerization (5). DsbA is reoxidized by the quinone reductase DsbB from the inner membrane, which generates disulfides *de novo* by the reduction of ubiquinone or menaquinone (2–4, 29, 55). The genes coding for the DsbA and DsbB proteins of the disulfide bond–formation system are usually not adjacent, but rather are located distant from each other on the genome of gram-negative bacteria (Fig. 3). However, certain bacteria contain genes encoding additional, homologous thiol/disulfide oxidases. For example, *Neisseria meningitidis* contains one DsbB gene and three homologous DsbA proteins (62, 71) presumed to act on distinct subsets of substrates.

Although most commensal *E. coli* strains contain only one *dsbA* and *dsbB* gene located distantly on the genome, the prototypic uropathogenic *E. coli* strain CFT073 (73) and other uropathogenic *E. coli* strains (51) contain an additional pair of redox proteins homologous to DsbA and DsbB, termed DsbL and DsbI, respectively, which are 19% and 24% identical to DsbA and DsbB of CFT073 (22). In contrast to the *dsbA* and *dsbB* genes, *dsbL* and *dsbI* are clustered together under the control of the same promoter in a single operon. Interestingly, this operon is tri-cistronic and also contains the gene encoding ASST (*astA*) that precedes the *dsbL* and *dsbI* genes (Fig. 3). The

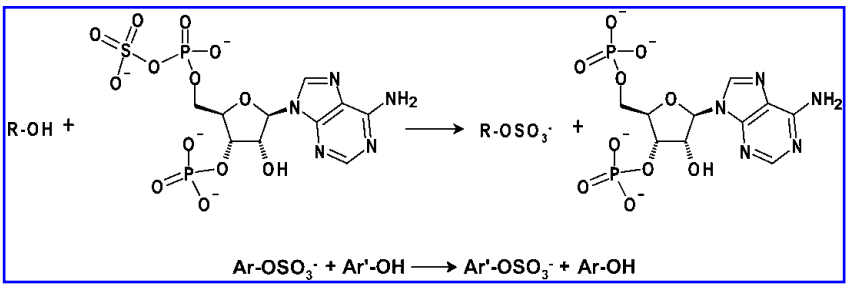

FIG. 1. Catalysis of sulfotransfer by PAPS-dependent and aryl sulfotransferases. PAPS-dependent sulfotransferases catalyze the transfer of a sulfuryl group from the "universal" sulfuryl donor PAPS, which is an anhydride, onto a variety of acceptors (*top*). The PAPS-independent aryl sulfotransferases catalyze sulfotransfer from one phenolic compound to another (Ar and Ar′ represent an aromatic moiety; *bottom*).

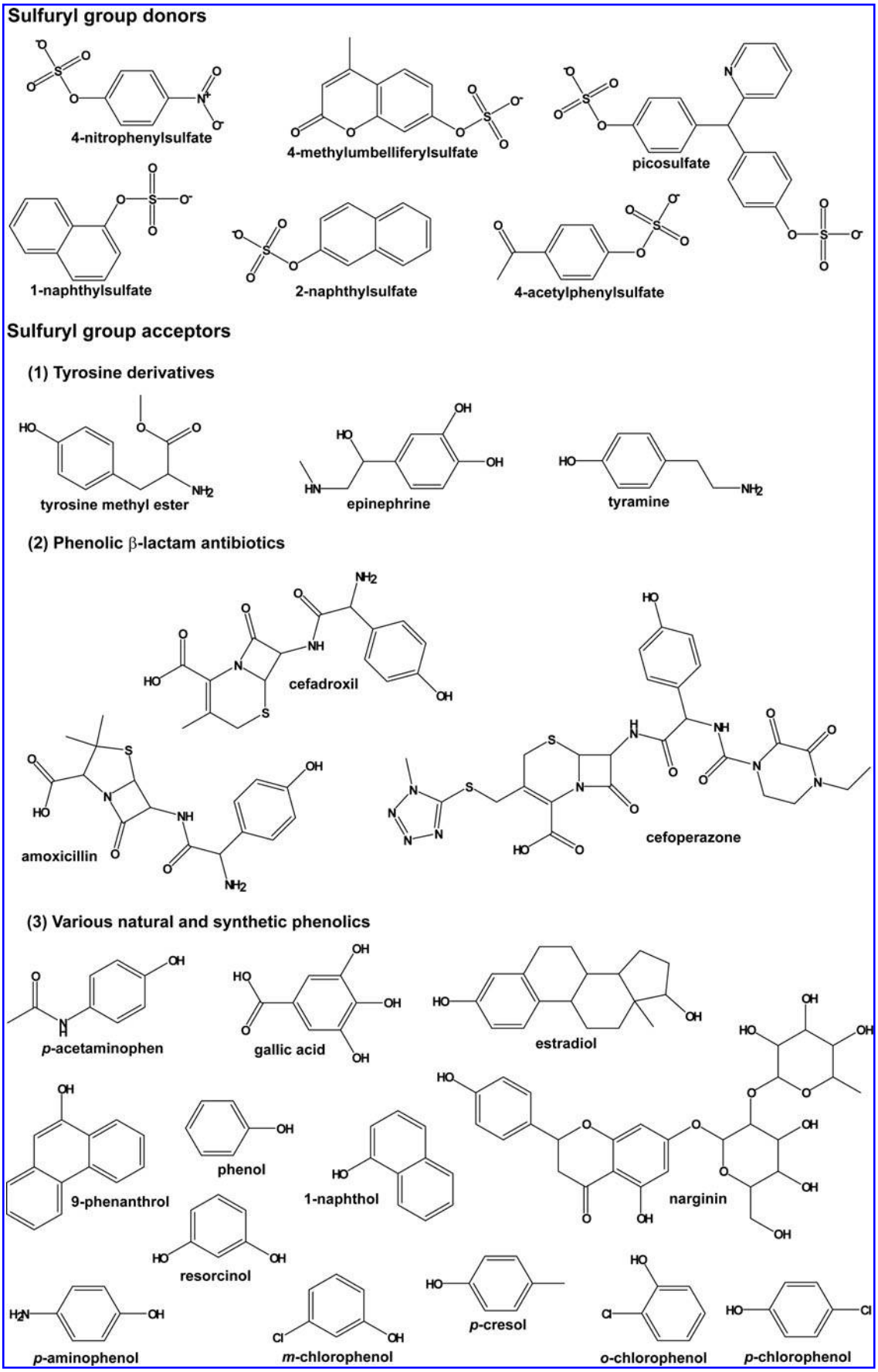

FIG. 2. An overview of molecular structures of phenolic sulfuryl donor and acceptor substrates for aryl sulfotransferases described in the literature.

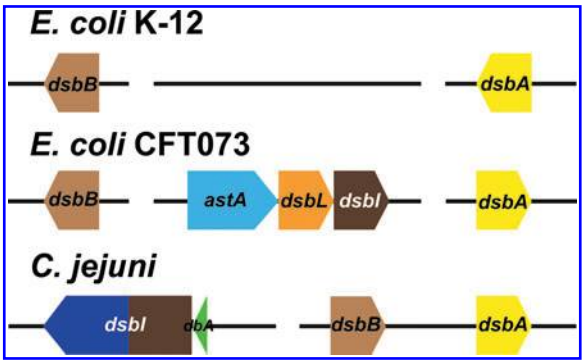

FIG. 3. Organization of the disulfide bond–formation pathway genes in *Escherichia coli* K12 (*top*), *E. coli* CFT073 (middle), and *Campylobacter jejuni* (*bottom*). These illustrate the genomic context of ASST. *Escherichia coli* K12 contains one gene for *dsbB* (*brown*) and one for *dsbA* (*yellow*), far apart on the genome, as does the *E. coli* CFT073. However, the CFT073 strain contains an additional homologue of each of them, *dsbL* (*orange*) and *dsbI* (*dark brown*), clustered together in the same operon with the *astA* gene (*blue*) encoding ASST. In *Campylobacter jejuni*, however, in addition to the *dsbB* and *dsbA* genes, a dicistronic operon codes for a peptide of 55 residues (*dbA*, *green*) and a large *dsbI* gene is found whose first segment is homologous to DsbB-like transmembrane oxidoreductases (*dark brown*); the latter is predicted to fold into a β-propeller (*dark blue*). Genes and intergenic regions are drawn to scale. A broken line indicates a large genome segment between the depicted genes. (For interpretation of the references to color in this figure legend, the reader is referred to the web version of this article at www.liebertonline.com/ars).

DsbL/DsbI redox couple forms a specific dithiol oxidase system generating the single disulfide bond in each subunit of the ASST homodimer *in vivo* (see later), which is directly introduced by DsbL, one of the most oxidizing thioredoxin-like proteins described to date (−95 mV) (22). The recently elucidated, high-resolution crystal structure of reduced DsbL revealed an extensive patch of positively charged residues around its active-site cysteines. In contrast to DsbL, its two structurally closest homologues, the generic dithiol oxidases *E. coli* DsbA (56) and *Vibrio cholerae* TcpG (27), both have a hydrophobic groove instead of the basic region. This basic groove is likely to govern the substrate specificity of DsbL-like dithiol oxidoreductases. During introduction of disulfide bonds into substrates, DsbA and TcpG are assumed to interact with multiple unfolded proteins with exposed hydrophobic patches. By contrast, the presence of the basic groove in DsbL may be indicative of a narrower substrate specificity, which is also supported by the observation that DsbL only partially complements *dsbA*$^-$ deficiency in *E. coli* K12 strains (22). The substrate specificity of DsbL toward ASST can be rationalized by multiple negative charges in the primary structure of ASST around its two disulfide-bonded cysteines (Cys^{418} and Cys^{424}). The polypeptide chain between Asp^{410} and Thr^{432} of ASST bears a net negative charge of −4 and is therefore complementary to the positively charged patch around the active-site cysteines in DsbL.

Because several excellent reviews on the mechanism and diversity of disulfide bond–formation systems in various bacteria have appeared recently (2, 25, 28, 32, 53), we focus on the structure and mechanism of ASST and the dependence of its biogenesis on DsbL and DsbI. The gene coding for ASST is present in bacteroidetes, firmicutes, and enterobacteria, as well as in γ-, δ-, and ε-proteobacteria, and is frequently found to encode periplasmic proteins with N-terminal signal sequence (22). Almost all known periplasmic ASSTs contain the conserved cysteine residues Cys^{418} and Cys^{424} (numbered according to the mature form of ASST from *E. coli* CFT073) that form a structural disulfide bond that is essential for ASST activity (22). Notably, all genomes encoding ASSTs with this structural disulfide bond invariably contain at least an adjacent *dsbL* gene, and most also contain a *dsbI* gene (22).

A tri-cistronic *astA-dsbL-dsbI* operon is present in pathogenic *E. coli* strains associated with extra-intestinal infection (the *E. coli* strains CFT073, 536, UTI89, and F11), avian pathogenic *E. coli*, and strains of *Salmonella*, *Shewanella* and *Campylobacter*. Interestingly, the pathogens *Campylobacter jejuni* and *Helicobacter pylori* contain an operon analogous to *astA-dsbL-dsbI* of uropathogenic *E. coli*. This operon encodes a short peptide (termed DbA for **Ds**b-**a**ccessory) lacking cysteine residues, followed by a large DsbB-like protein (47, 73) (Fig. 3). This homologue of DsbB, termed DsbI, is significantly larger than *E. coli* DsbB. Its N-terminal segment contains the DsbB-like fold including the CXXCXXXR motif at the beginning of the second transmembrane helix, which is responsible for *de novo* disulfide-bond formation in *E. coli* DsbB after oxidation of the cysteine pair with quinones (55, 77), whereas the second cysteine pair, present in DsbBs, is absent in this DsbI. An additional, fifth transmembrane helix connects this N-terminal DsbB-like part with a periplasmic, C-terminal domain with a predicted β-propeller fold similar to that of ASST (see later) (47, 64). Homologues of this periplasmic domain are present almost exclusively in the strains of *Campylobacter* and *Helicobacter* and only a few other genera of γ- and ε-proteobacteria, like *Shewanella*, *Marinobacter*, *Pantoea*, *Vibrio*, *Aggregatibacter*, *Photobacterium*, and *Pasteurella*; its homology with any other characterized protein is marginal (47). Hence, this *dbA-dsbI* system may resemble the *astA-dsbL-dsbI* system of *E. coli* CFT073, where a large protein exhibiting the β-propeller fold (ASST) is related to a disulfide bond–generation system.

Although the biologic function of ASST still remains to be determined, genetic data suggest a role for ASST in virulence. Its gene is one of the few genes identified to be specific for uropathogenic *E. coli* strains (51). ASST from the uropathogenic *E. coli* strain CFT073 (73), isolated from the blood of a patient with acute pyelonephritis and cytotoxic to human renal cells (58), was found upregulated in a mouse model of a urinary tract infection (51). Because ASST sulfurylates a number of phenolic compounds, it was suggested to be involved in sulfur uptake, detoxification of phenolic compounds, and antibiotic resistance (42). In addition, numerous examples of specialized redox proteins besides DsbA and DsbB exist in pathogenic organisms, which participate in folding of specific, virulence-related substrates. These include the plasmid-encoded DsbA homologue SeSrgA in *Salmonella enterica* subsp. *enterica serovar Typhimurium*, which catalyzes the folding of subunits of plasmid-encoded fimbriae (7). Another interesting example is the DsbA homologue BdbB in the gram-positive organism *Bacillus subtilis*, required for the biogenesis of the antibiotic peptide lantibiotic sublancin 168, in which both the *sunA*

gene encoding the sublancin 168 lantibiotic antimicrobial precursor peptide and the *bdbB* gene are separated by only three genes on the genome (15). Just as SeSrgA and BdbB help fold specific virulence factors in *S. enterica* and *B. subtilis*, respectively, the genes encoding bacterial periplasmic ASSTs are often found clustered with the genes coding for the DsbL and DsbI proteins homologous to the disulfide bond–formation proteins DsbA/DsbB. Furthermore, the previously mentioned DsbI in *H. pylori*, which contains a *bona fide* ASST-like periplasmic domain, is required for this bacterium to colonize gastric mucosa (20).

At present, the relation of ASST-DsbL-DsbI to bacterial virulence remains to be established. Genetic data have demonstrated that of all *E. coli* strains, these proteins are found specifically in the uropathogenic members and are upregulated in the urinary tract infection model (51). Conversely, however, some recent *in vivo* studies did not confirm a role for ASST in virulence (50, 70). Further experiments will thus be required to clarify the exact *in vivo* role of ASST and its possible relation to urinary tract infection.

Molecular Structure and Catalytic Mechanism of Aryl Sulfotransferase from Uropathogenic *Escherichia coli* CFT073

Overall molecular structure of aryl sulfotransferase

Until very recently, no structural information other than the oligomerization state was available on bacterial aryl sulfotransferases. For example, ASST from *Klebsiella* K-36 was described as a homodimer (1), whereas the *Enterobacter amnigenus* AR-37 ASST was found to be monomeric (45), and *Eubacterium* A-44 was reported to be tetrameric (44).

In 2008, however, three crystal structures of ASST from *E. coli* CFT073 (Fig. 4) were reported, including the enzyme in its free form [Protein Data Bank (PDB) accession number: 3ELQ], and two structures of the sulfo-enzyme state (PDB accession numbers: 3ETS and 3ETT) representing a catalytic intermediate in the reaction cycle of the enzyme (54).

Arylsulfate sulfotransferase from *E. coli* CFT073 is a homodimeric protein, both in solution and in the crystal. According to the *E. coli* Cell Envelope Protein Data Collection (http://www.cf.ac.uk/biosi/staffinfo/ehrmann/tools/ecce/ecce.htm; accessed 20 Dec 2009), the 571-residue ASST monomer (63,763 Da) belongs in the top 10% of the largest polypeptide chains in the periplasm of *E. coli.* Each ASST monomer consists of two domains: a small N-terminal domain (residues 1–116), forming a seven-stranded β-sandwich, followed by a large C-terminal domain (residues 117–571) (Fig. 4A and B). The C-terminal domain folds into a six-bladed β-propeller formed by the packing of six four-stranded β-sheets in a circular array around a central cavity.

In common with most other β-propeller structures, the channel formed by the blades of the propeller is conical (61). This channel narrows in diameter from $\sim$21 Å on the surface to $\sim$10 Å in the region of the active site, is solvent accessible, and is suitable for substrate sequestration. A disordered loop (residues Val^{321}–Leu^{327}) flanks the channel entrance. The loop's poorly defined electron density points to a high degree of flexibility, presumably facilitating free passage of substrates to the interior of the enzyme.

Interestingly, proteins belonging to the β-propeller fold are most frequently found in eukaryotic organisms, where their roles span RNA processing, transcription regulation, cytoskeleton assembly, mitotic-spindle formation, vesicle formation, and trafficking (67). The known bacterial β-propeller folds are usually enzymes, most frequently redox enzymes or esterases (31). ASST from *E. coli* CFT073 also catalyzes the chemical transformation of esters.

Architecture of the active site of ASST

Initial work on the catalytic mechanism of ASSTs suggested that the enzyme becomes transiently sulfurylated at a tyrosine residue (corresponding to Tyr^{96} in ASST from *E. coli* CFT073) in its active site after interaction with the donor substrate, followed by the transfer of the sulfuryl group to the acceptor (46). However, no additional electron density around Tyr^{96} ASST from *E. coli* CFT073 could be identified in crystals soaked with donor or acceptor compounds. Crystals of free ASST, obtained with lithium sulfate as a precipitant, contain several sulfate groups, most of which likely act as counterions to a positively charged amino acid side chain at the protein surface. However, a sulfate ion adjacent to His^{436} at the bottom of the central β-propeller channel of ASST was bound in a very specific and unusual manner. This sulfate was situated in the central channel of the β-propeller and participated in an extensive hydrogen-bond network with the nitrogen atoms of five neighboring side chains, His^{252}, His^{356}, Asn^{358}, Arg^{374}, and His^{436}, and the backbone nitrogen of Thr^{501} (Fig. 4C and Fig. 5). This complex network of hydrogen bonds, together with a comparison of the location of the active site in other enzymes exhibiting a β-propeller fold (61), suggested that the central channel of the ASST β-propeller fold bears the active site. This assumption was subsequently confirmed by the structures of ASST in complex with substrates and by mass spectrometry, kinetic studies, and site-directed mutagenesis experiments (see later).

The structures of ASST obtained on crystal soaking with the sulfuryl donor substrates *p*-nitrophenylsulfate (PNS) and 4-methylumbelliferylsulfate (MUS) indeed revealed these two compounds to be bound in the center of the β-propeller, and ASST was found to be covalently sulfurylated on the $N^{\varepsilon 2}$ atom of the residue His^{436}. Whereas the structure of the substrate-free enzyme contains an ordered sulfate group at the equivalent position (see earlier), the structures with MUS and PNS exhibited continuous electron density from the $N^{\varepsilon 2}$ atom of His^{436} to the sulfuryl group, and the center of this density was $\sim$1 Å closer than in the structure with a sulfate ion bound, in agreement with a covalent nitrogen–sulfur bond. In these structures, which represent trapped sulfurylated reaction intermediates of ASST, desulfurylated donor compounds remained bound in the active-site cleft, whereas the sulfuryl moiety of sulfohistidine was stabilized by extensive hydrogen bonding to the side chains of His^{252}, Asn^{358}, Arg^{374}, His^{356}, and the backbone nitrogen of Thr^{501} (Fig. 4D and E and Fig. 5). The hydroxyl groups of the desulfurylated donors form a hydrogen bond with the sulfo-His^{436} and a hydrophobic contact with the residue Phe^{171}.

The only segment in the ASST structure without detectable electron density comprised residues Val^{321}–Leu^{327}, which are relatively close to the active site and may contribute to the specific recognition of natural ASST substrates.

In accordance with the crystallographic observations, structure-based sequence alignment of ASST homologues

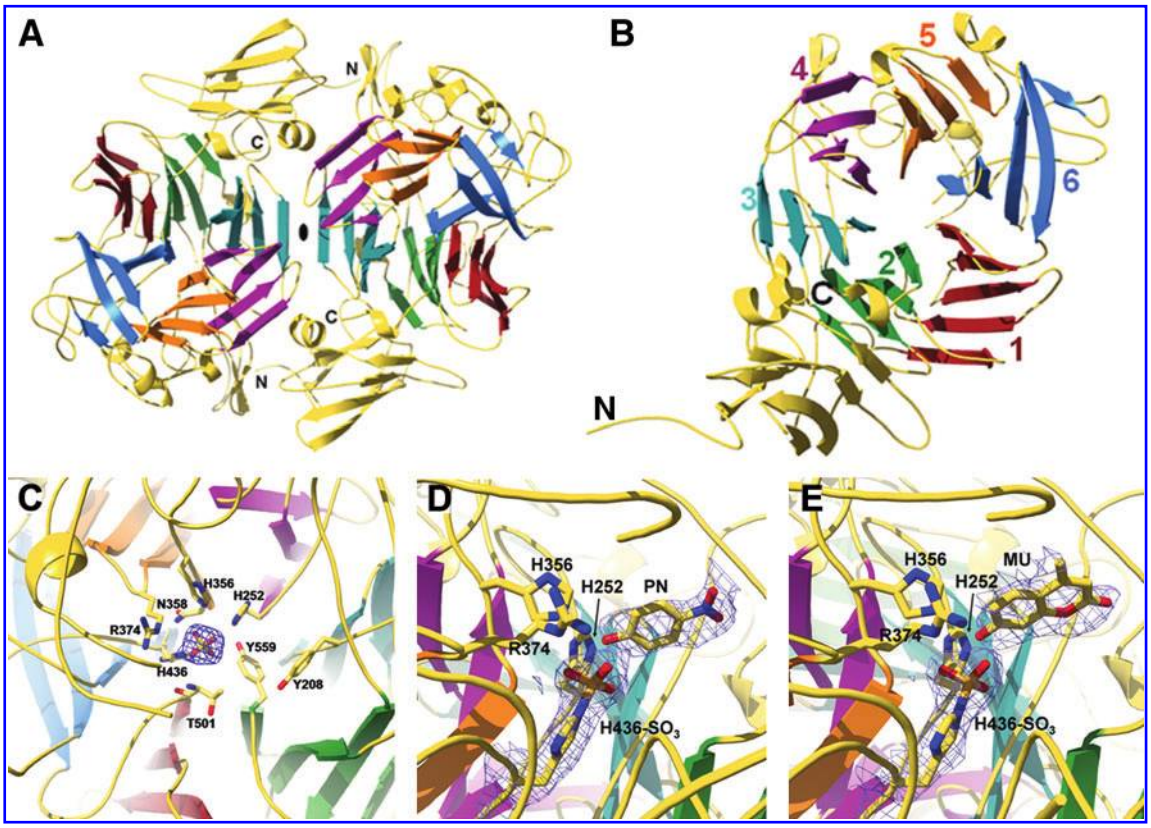

FIG. 4. Crystal structure of ASST. (**A**) Top view along the two-fold noncrystallographic symmetry axis, which relates the two monomers. (**B**) Each monomer consists of a small, N-terminal seven-stranded β-sandwich domain, and a larger C-terminal, six-bladed β-propeller domain. (**C**) The structure of substrate-free ASST exhibits a sulfate dianion that is coordinated by nitrogen atoms from the active-site residues His^{252}, His^{356}, Asn^{358}, Arg^{374}, His^{436}, and the backbone nitrogen of Thr^{501}. Both structures of ASST obtained from crystals soaked with *p*-nitrophenol (PNS) (**D**) and 4-methylubelliferysulfate (MUS) (**E**) show His^{436} to be sulfurylated at its $N^{\varepsilon 2}$ atom, whereas the desulfurylated donors (*p*-nitrophenol and 4-methylumbelliferone, respectively) are located in the central channel of the β-propeller. Electron density is shown and contoured at 1.5 σ. (For interpretation of the references to color in this figure legend, the reader is referred to the web version of this article at www.liebertonline.com/ars).

(Fig. 5) revealed all active-site residues (His^{252}, His^{356}, Arg^{374}, and His^{436}) to be invariant. In addition, the only invariant segment of more than three consecutive residues throughout the whole protein sequence in all ASST homologues analyzed corresponded to the pentapeptide sequence Tyr^{434}-Ala^{438}, centered at His^{436}. Furthermore, the residues around His^{436} in the three-dimensional structure of ASST undergo purifying selection [*i.e.,* across-species mutations of the corresponding codons are less likely to be residue changing than silent (16)], in agreement with their critical role in catalysis (54).

A very recent study (68) compared and contrasted the active-site architectures of the PAPS-dependent sulfotransferase mSULT1D1 (69) and ASST (54). PAPS-dependent sulfotransferases catalyze sulfuryl transfer from the donor PAPS onto an acceptor (with a hydroxyl or an amino group) by simultaneous binding of donor and acceptor in an orientation favoring sulfotransfer. An invariant active-site histidine residue in PAPS-dependent sulfotransferases activates the acceptor group to attack the sulfuryl group of the donor, and the transfer occurs directly, without transient sulfurylation of the enzyme (10). Conversely, the active site of ASST can accommodate either the donor or the acceptor compound, but both cannot be bound simultaneously. The catalysis proceeds through transient sulfurylation of the enzyme on its active-site histidine residue, which subsequently sulfurylates the acceptor compound. A comparison of the active sites of a PAPS-dependent mSULT1D1 and ASST, both in complex with 4-nitrophenol (which acted as the acceptor substrate in the structure of the PAPS-dependent sulfotransferase, whereas it represented the desulfurylated donor substrate in the case of ASST) revealed a striking similarity in the architecture of both enzymes' active sites (Fig. 6). Interestingly, both classes of sulfotransferases exhibit a nearly identical spatial arrangement of active-site residues, which not only applies to the residues directly involved in catalysis, but also to those governing substrate recognition. Furthermore, the sulfuryl group to be transferred is oriented identically toward the acceptor substrate in both structures. This demonstrates a high degree of similarity of the sulfotransfer chemistry in both enzyme classes, despite their very different overall fold, indicating a significant degree of convergent evolution of both classes of enzymes.

Biochemical and mechanistic studies of ASSTs

Most biochemical studies performed on ASSTs from several organisms revealed that ASST is able to use a variety of phenolic sulfates as sulfuryl-donor compounds as well as a

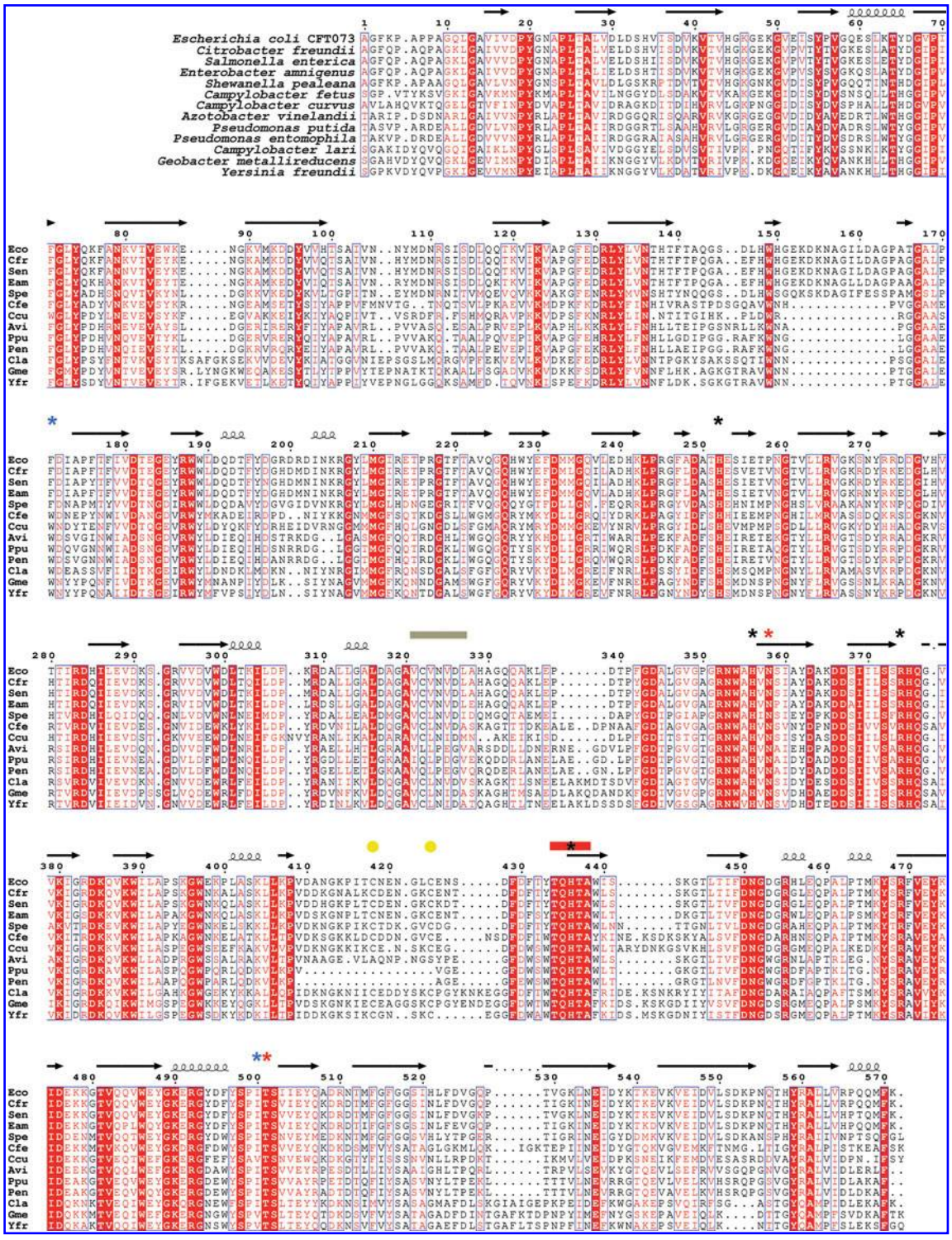

FIG. 5. Structure-based sequence alignment of ASSTs. Residues are numbered according to mature ASST from *E. coli* CFT073. Conserved residues are boxed in red. The sequences from *E coli* CFT073, *Citrobacter freundii*, *Salmonella enterica*, *Enterobacter amnigenus*, *Shewanella pealeana*, *Campylobacter fetus*, *Campylobacter curvus*, *Azotobacter vinelandii*, *Pseudomonas putida*, *Pseudomonas entomophila*, *Campylobacter lari*, *Geobacter metallireducens*, and *Yersinia freundii* were aligned. Depicted are the floppy hinge region that covers the active site (gray bar), the longest invariant segment centered at the catalytic residue His^{436} (red bar), the structural cysteines (yellow circles), as well as the active-site residues (asterisks). Black asterisks denote the central residues that are capable of (de)protonating the substrate; red asterisks represent those involved in hydrogen bonding of the sulfuryl group in the active site; and grey asterisks indicate residues forming hydrophobic contact with the aromatic moiety of the substrate. (For interpretation of the references to color in this figure legend, the reader is referred to the web version of this article at www.liebertonline.com/ars).

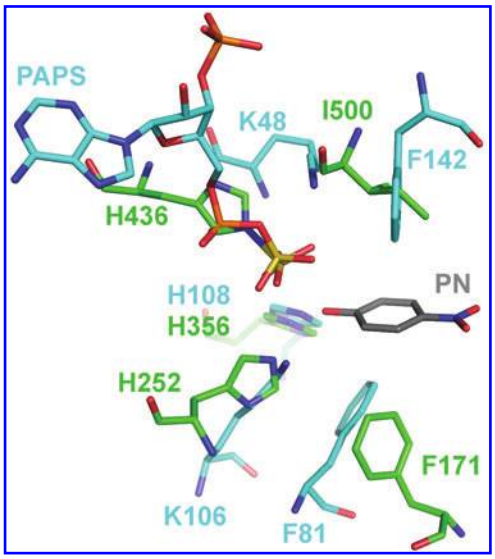

FIG. 6. Overlay of the active-site residues of ASST (PDB: 3ETT) and the PAPS-dependent sulfotransferase mSULT1D1 (PDB ID: 2ZYV), both in complex with *p*-nitrophenol (PN), which was used as a reference to superimpose the two protein structures. Nitrogen and oxygen atoms are depicted in blue and red, respectively, whereas the carbon atoms from active-site side chains of ASST and mSULT1D1 are shown in green and cyan, respectively, and the carbon atoms of PN are depicted in grey. The single-letter amino acid code is used (I, isoleucine; F, phenylalanine; H, histidine, K, lysine). (For interpretation of the references to color in this figure legend, the reader is referred to the web version of this article at www.liebertonline.com/ars).

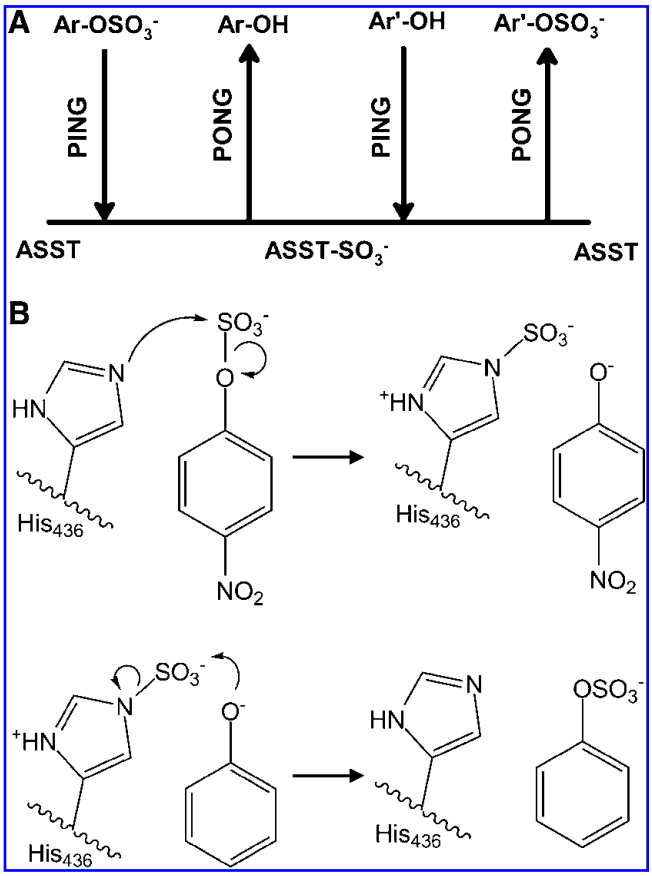

FIG. 7. ASST from *Escherichia coli* CFT073 shows a ping-pong bi-bi reaction mechanism (A) with transient formation of a sulfohistidine (B). During the first step of catalysis, the free electron pair of $N^{\varepsilon 2}$ from His^{436} nucleophilically attacks the sulfur atom of a phenolic donor compound (here, *p*-nitrophenylsulfate), yielding a covalent sulfohistidine intermediate and *p*-nitrophenylate. After dissociation of *p*-nitrophenylate and binding of phenol, the phenolate oxygen of an acceptor (here phenol) nucleophilically attacks the sulfur in the intermediate, and the sulfhydryl group is transferred onto the acceptor.

variety of phenols as acceptors (depicted in Fig. 2). In addition, the kinetic characterization of ASST from *Eubacterium* A-44, with the substrates PNS and tyramine, demonstrated a ping-pong bi-bi reaction mechanism (39). The catalytic cycle consists of two steps and begins with the binding of the donor compound into the active-site pocket ("ping"), followed by sulfurylation of the enzyme and the release of the phenolic donor ("pong"). The second step includes binding of the acceptor substrate, transfer of the sulfuryl group to the acceptor, and the release of the sulfurylated acceptor (Fig. 7). The ping-pong bi-bi mechanism identified in ASST is frequently observed in other transferases (13, 39, 63, 72). Nevertheless, different models for the individual microscopic steps during the catalytic cycle of ASST were initially proposed. A first study suggested that the catalysis proceeds through the transient sulfurylation of a tyrosine residue in ASST, possibly because tyrosine is the only amino acid with a phenolic side chain, which resembles the phenolic donor and acceptor compounds. Therefore, its sulfurylation would not produce intermediates of significantly different chemical stability than the reactants or products (all would be phenolic sulfates). Thus, site-directed mutagenesis studies were aimed at replacing tyrosines with phenylalanines and measuring the catalytic activity of the resulting variants. For example, Kwon *et al.* (46) reported that the replacement $Tyr^{123}Phe$ in *Enterobacter amnigenus* ASST (this numbering of residues includes the periplasmic signal sequence, not the mature protein) reduced the catalytic activity to $< 4\%$ of the wild type and proposed this tyrosine to be the residue undergoing transient sulfurylation. Another study on ASST from *Eubacterium* A-44 ASST (41) demonstrated that the histidine-modifying compound diethylpyrocarbonate (DEPC) (65) inactivates the enzyme, suggesting that a histidine residue is essential for catalysis. In addition, an elegant infrared spectroscopy study on the same *Eubacterium* A-44 ASST (9) demonstrated that the absolute stereochemical configuration at sulfur remains preserved during catalysis rather than being inverted, which implied an odd number of covalent sulfo-enzyme intermediates. From all studies, it was finally suggested that tyrosine is the only residue undergoing covalent modification by the sulfuryl group, and the histidine residue acts as a general acid–base catalyst activating the catalytic tyrosine (9).

The crystal structures of substrate-free ASST from *E. coli* CFT073 and its catalytic intermediates with substrates bound, described earlier, provided direct insight into catalysis, and, complemented with biochemical experiments described later, enabled the exact formulation of the reaction mechanism.

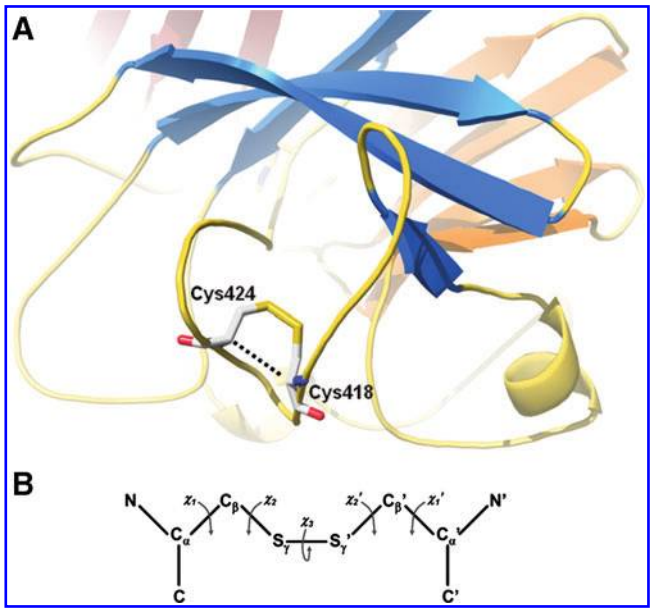

FIG. 8. The disulfide bond Cys^{418}-Cys^{424} of ASST shows unusual geometry. (**A**) The single disulfide bond in ASST is situated in a loop in the outer part of blade 6 of the propeller. The C_α (Cys^{418})–C_α (Cys^{424}) distance (*dashed line*) is only 3.82 Å. The same color scheme as in Fig. 3 is used. (**B**) Dihedral angles of a disulfide bond. The values for the Cys^{418}-Cys^{424} disulfide in ASST are as follows: χ_1, −37.1 degrees; χ_2, −110.9 degrees; χ_3, 86.5 degrees; χ_2', −77.7 degrees; and χ_1', −53.9 degrees. The angle χ_1 is defined by the planes of (N, C_α, C_β) and (C_α, C_β, and S_γ). (For interpretation of the references to color in this figure legend, the reader is referred to the web version of this article at www.liebertonline.com/ars).

First, the replacement of individual residues in the center of the β-propeller suspected to be involved in catalysis and the comparison of the sulfotransferase activity of the corresponding ASST variants with that of the wild type revealed that the replacement of Arg^{374}, His^{252}, or His^{356} dramatically impaired ASST activity, to 0.1%, 4.0%, and 0.06%, respectively, suggesting that these residues are critically important for catalysis. In contrast, the activity of the point variants Tyr^{208}Phe and Tyr^{559}Phe and of the double variant Tyr^{208}-Phe/Tyr^{559}Phe was comparable to that of the wild type, indicating that these tyrosines do not participate in catalysis. As Tyr^{208} and Tyr^{559} are the only tyrosines in the substrate-binding pocket of ASST, transient sulfurylation of tyrosines could be excluded. Similarly, replacement of Tyr^{96}, the initially proposed catalytic ASST residue (46), had no effect on activity (54). These data strongly support a mechanism in which a sulfurylated active-site histidine directly delivers the sulfuryl group to the aromatic hydroxyl group of an acceptor substrate. The desulfurylation of the sulfohistidine intermediate of ASST can thus be regarded as a simple inverse of ASST sulfurylation by a donor, whereby the active-site residues His^{252}, His^{356}, and Arg^{374} provide a means for coordination of the sulfuryl moiety during the catalytic cycle (Fig. 4) (8, 21, 54).

Second, the essential role of the histidines in the active site of ASST from *E. coli* CFT073 was further confirmed by inactivation of ASST through treatment with diethylpyrocarbonate (DEPC). In contrast, reagents such as iodoacetamide and PMSF, targeting thiol and nucleophilic hydroxyl groups, respectively, had no influence on ASST activity (54).

Third, mass spectrometric data are in keeping with the covalent sulfurylation of His^{436} during its catalytic cycle. The electrospray ionization mass spectra of freshly purified ASST exhibited two peaks, one at 63,764.5 ± 2 Da, the mass expected for the monomer, and a second one of similar intensity at 63,845.5 ± 2 Da. Incubation of this ASST preparation with the sulfuryl acceptor phenol resulted in the disappearance of the higher-molecular-weight peak. Conversely, the treatment of this desulfo-ASST with the sulfuryl donor PNS restored the higher-molecular-weight peak. The mass difference of the two peaks of 80 ± 2 Da confirmed the covalent modification of the protein by the $-SO_3^-$ group. In addition, the formation of sulfurylated His^{436} was confirmed by the tryptic digestion of sulfurylated ASST followed by mass spectrometry of tryptic ASST peptides, where only the peptide Leu^{405}–Lys^{443}, bearing His^{436}, appeared as a double peak with a characteristic mass difference of 80 Da. This further confirmed that His^{436} is the sulfurylated residue in the ASST fragment, as His^{436} is the only histidine residue within this tryptic ASST peptide (54).

Fourth, steady-state kinetics performed by using 4-methylumbelliferylsulfate as the donor substrate and phenol as the acceptor substrate confirmed the ping-pong bi-bi mechanism and also revealed substrate inhibition by the acceptor phenol (see later). The catalytic constant k_{cat} remains essentially constant in the pH range from 6.0 to 10.0, whereas the Michaelis constant for the donor increases and the Michaelis constant for the acceptor decreases with increasing pH (54). The kinetic parameters obtained for ASST at pH 8 are: Michaelis constant for the donor MUS, $K_{M,MUS} = (4.45 \pm 0.72)\ 10^{-5}\ M$; Michaelis constant for the acceptor phenol $K_{M,phenol} = (1.35 \pm 0.19) \times 10^{-3}\ M$, inhibition constant for the acceptor phenol $K_{I,phenol} = (1.13 \pm 0.22)\ 10^{-3}\ M$, and the catalytic constant $k_{cat} = (48.6 \pm 0.5)$ per second. These values indicated that ASST is an enzyme of average catalytic efficiency (72).

The acceptor substrate phenol proved to inhibit ASST activity significantly at pH values of ≥ 8.0, whereas inhibition by phenol was negligible at lower pH values. Substrate inhibition is predicted for the ping-pong bi-bi mechanism outlined in Fig. 7, as both donor and acceptor substrate mutually exclude each other when bound to the same active site and are of similar chemical structures (phenolic anions). The pronounced substrate inhibition by phenol at higher pH values suggests that the actual inhibitor is the phenolate anion [pK_a(phenol/phenolate) = 9.95 (49)], and demonstrates that the active site in substrate-free ASSTs recognizes anionic phenolic compounds. The donor substrates (phenolic sulfates) are indeed negatively charged at physiologic pH values.

Taken together, a wealth of independent experimental data support the ping-pong bi-bi reaction mechanism of ASST from *E. coli* CFT073. The residue His^{436} undergoes transient covalent sulfurylation during the catalytic cycle as depicted in Fig. 7. The transition state of the catalysis most likely includes a pentacoordinated sulfur atom, with the three oxygen atoms of the sulfuryl group defining the equatorial positions of a trigonal bipyramid, whereas one apex is defined by the oxygen of the donor or acceptor, and the other, by the $N^{\varepsilon 2}$ nitrogen of His^{436}. The overall negative charge of the transition state is probably stabilized by the positively charged side chain of Arg^{374} and possibly also by His^{252} and His^{356}.

The unusual disulfide bond in ASST

As mentioned earlier, the two conserved cysteines, Cys^{418} and Cys^{424} of ASST, form a structural disulfide bond that is essential for ASST folding. This disulfide bond is located in a loop in the outer part of the sixth propeller blade and shows a very unusual geometry (Fig. 8). The distance between the two C_α atoms of the cysteines is only 3.8 Å, which is extremely short as compared with the mean of 5.63 Å for all protein disulfides (52, 66). The dihedral angles of this disulfide (χ_1, χ_2, χ_3, χ_2', and χ_1' with the signs −, −, +, −, and −, respectively) classify it into the so-called right-handed staple (–RHStaple) geometry. The high dihedral strain energy predicted for this bond [estimated at ∼30 kJ/mol (52)] may be overcome by additional interactions stabilizing the ASST tertiary structure that require formation of the Cys^{418}-Cys^{424} bond. Interestingly, bioinformatic analyses revealed that strained, high energy disulfides, like the Cys^{418}-Cys^{424} in ASST, often play a regulatory role in protein function, triggering a conformational change when they break or form (17). Such disulfides typically have a high torsional strain energy (23) and are often found on adjacent β-strands (24, 74). A well-studied example is the -RHStaple disulfide in the tissue factor involved in the regulation of hemostasis, and several other similar disulfides have been described (11, 12, 26, 66). This relatively rare class of strained disulfides is statistically overrepresented in proteins involved in cell entry, like bacterial toxins and viral entry proteins [this topic is comprehensively reviewed in (75)]. The conserved disulfide Cys^{418}-Cys^{424} in ASST is close to the surface of the protein and may be accessible to regulation by external factors. Furthermore, it is situated in the same propeller blade, just 12 residues before the catalytic residue His^{436}, which undergoes transient sulfurylation in the ASST reaction, and may influence conformational equilibria in ASST.

A possible explanation for the dependence of oxidative ASST folding on DsbL (22) could be that the ASST segment containing the Cys^{418}/Cys^{424} pair may become rapidly inaccessible to the generic dithiol oxidase DsbA after initiation of ASST folding in the periplasm. DsbL has, however, been shown to possess a high-affinity binding site for unfolded polypeptides, as it prevents unspecific aggregation of reduced insulin (22). This chaperone-like activity may help to maintain ASST in an unfolded conformation that allows disulfide exchange between DsbL and ASST, or to recycle oxidation-incompetent, dead-end folding intermediates of ASST. In addition, the highly oxidizing active-site disulfide of DsbL, with a redox potential of −95 mV compared with −121 mV for DsbA (76), may further facilitate introduction of the disulfide bond into ASST folding intermediates.

Conclusion and Outlook

Aryl sulfotransferases from a range of different prokaryotic organisms have recently been characterized (1, 33–35, 37, 38, 45, 46, 54), demonstrating an increasing interest in this class of enzymes. These enzymes have attracted scientific attention because of their potential role in infectious diseases, especially urinary tract infections, and, conversely, because of their dependence on DsbL as an alternative catalyst of disulfide bond formation.

The recently elucidated crystal structure of ASST from *E. coli* CFT073 and its catalytic intermediates, with substrates bound to the active site, provided a framework for understanding the molecular basis of PAPS-independent sulfotransfer. In addition, ASSTs are the only enzymes known that make use of a high-energy sulfohistidine intermediate during their reaction cycle. PAPS-independent sulfotransferases with activities similar to those of ASSTs have so far not been identified in eukaryotes, but it remains to be established whether these enzyme occur exclusively in prokaryotes.

The most important unsolved problem in research on ASSTs is certainly the elucidation of their biologic function and their potential role in pathogenesis. The identification of natural ASST substrates and further genetic studies and *in vivo* experiments will be required to uncover the role of ASST in infectious diseases and to establish ASSTs as potential drug targets. High-throughput computational docking and molecular modeling may help to identify natural sulfuryl donor and acceptor substrates and should be paralleled by structure-based design of specific inhibitors and testing of fractionated body fluids for the presence of substrates. Because of their relatively broad substrate specificity *in vitro*, ASSTs may also be useful for the synthesis of sulfophenols and for quantitative measurements of equilibrium states of sulfotransfer reactions between aromatic sulfuryl donors and acceptors.

Acknowledgments

This work was supported by the Swiss National Science Foundation and the ETH Zurich within the framework of the National Center for Competence in Research Structural Biology program. We thank all current and past members of our group and collaborators for stimulating scientific discussions.

References

1. Baek MC, Kim SK, Kim DH, Kim BK, and Choi EC. Cloning and sequencing of the Klebsiella K-36 astA gene, encoding an arylsulfate sulfotransferase. *Microbiol Immunol* 40: 531–537, 1996.
2. Bardwell JC. Building bridges: disulphide bond formation in the cell. *Mol Microbiol* 14: 199–205, 1994.
3. Bardwell JC, Lee JO, Jander G, Martin N, Belin D, and Beckwith J. A pathway for disulfide bond formation in vivo. *Proc Natl Acad Sci U S A* 90: 1038–1042, 1993.
4. Bardwell JC, McGovern K, and Beckwith J. Identification of a protein required for disulfide bond formation in vivo. *Cell* 67: 581–589, 1991.
5. Berkmen M, Boyd D, and Beckwith J. The nonconsecutive disulfide bond of *Escherichia coli* phytase (AppA) renders it dependent on the protein-disulfide isomerase, DsbC. *J Biol Chem* 280: 11387–11394, 2005.
6. Bojarova P and Williams SJ. Sulfotransferases, sulfatases and formylglycine-generating enzymes: a sulfation fascination. *Curr Opin Chem Biol* 12: 573–581, 2008.
7. Bouwman CW, Kohli M, Killoran A, Touchie GA, Kadner RJ, and Martin NL. Characterization of SrgA, a *Salmonella enterica* serovar *Typhimurium* virulence plasmid-encoded paralogue of the disulfide oxidoreductase DsbA, essential

for biogenesis of plasmid-encoded fimbriae. *J Bacteriol* 185: 991–1000, 2003.
8. Cameron DR and Thatcher GRJ. Mechanisms of reaction of sulfate esters: a molecular orbital study of associative sulfuryl group transfer, intramolecular migration and pseudorotation. *J Org Chem* 61: 5986–5997, 1996.
9. Chai CL and Lowe G. The mechanism and stereochemical course of sulfuryl transfer catalysed by the aryl sulfotransferase from *Eubacterium* A-44. *Bioorg Chem* 20: 181–188, 1992.s
10. Chapman E, Best MD, Hanson SR, and Wong CH. Sulfotransferases: structure, mechanism, biological activity, inhibition, and synthetic utility. *Angew Chem Int Ed Engl* 43: 3526–3548, 2004.
11. Chen VM, Ahamed J, Versteeg HH, Berndt MC, Ruf W, and Hogg PJ. Evidence for activation of tissue factor by an allosteric disulfide bond. *Biochemistry* 45: 12020–12028, 2006.
12. Chen VM and Hogg PJ. Allosteric disulfide bonds in thrombosis and thrombolysis. *J Thromb Haemost* 4: 2533–2541, 2006.
13. Cook PF and Cleland WW. *Enzyme Kinetics and Mechanism*. London: Garland Science, 2007.
14. Devi VS, Sprecher CB, Hunziker P, Mittl PR, Bosshard HR, and Jelesarov I. Disulfide formation and stability of a cysteine-rich repeat protein from *Helicobacter pylori*. *Biochemistry* 45: 1599–1607, 2006.
15. Dorenbos R, Stein T, Kabel J, Bruand C, Bolhuis A, Bron S, Quax WJ, and Van Dijl JM. Thiol-disulfide oxidoreductases are essential for the production of the lantibiotic sublancin 168. *J Biol Chem* 277: 16682–16688, 2002.
16. Doron-Faigenboim A, Stern A, Mayrose I, Bacharach E, and Pupko T. Selecton: a server for detecting evolutionary forces at a single amino-acid site. *Bioinformatics* 21: 2101–2103, 2005.
17. Fan SW, George RA, Haworth NL, Feng LL, Liu JY, and Wouters MA. Conformational changes in redox pairs of protein structures. *Protein Sci* 18: 1745–1765, 2009.
18. Gamage N, Barnett A, Hempel N, Duggleby RG, Windmill KF, Martin JL, and McManus ME. Human sulfotransferases and their role in chemical metabolism. *Toxicol Sci* 90: 5–22, 2006.
19. Gibson KE, Kobayashi H, and Walker GC. Molecular determinants of a symbiotic chronic infection. *Annu Rev Genet* 42: 413–441, 2008.
20. Godlewska R, Dzwonek A, Mikula M, Ostrowski J, Pawlowski M, Bujnicki JM, and Jagusztyn-Krynicka EK. *Helicobacter pylori* protein oxidation influences the colonization process. *Int J Med Microbiol* 296: 321–324, 2006.
21. Graafland T, Wagenaar A, Kirby AJ, and Engberts JBFN. Structure and reactivity in intramolecular catalysis. catalysis of sulfonamide hydrolysis by the neighboring carboxyl group. *J Am Chem Soc* 101: 6981–6991, 1979.
22. Grimshaw J, Stirnimann CU, Brozzo MS, Malojcic G, Grütter MG, Capitani G, and Glockshuber R. DsbL and DsbI form a specific dithiol oxidase system for periplasmic arylsulfate sulfotransferase in uropathogenic *E. coli*. *J Mol Biol* doi:10 .1016/j.jmb.2008.05.031, 2008.
23. Haworth NL, Feng LL, and Wouters MA. High torsional energy disulfides: relationship between cross-strand disulfides and right-handed staples. *J Bioinformat Comput Biol* 4: 155–168, 2006.
24. Haworth NL, Gready JE, George RA, and Wouters MA. Evaluating the stability of disulfide bridges in proteins: a torsional potential energy surface for diethyl disulfide. *Mol Simulat* 33: 475–485, 2007.
25. Heras B, Shouldice SR, Totsika M, Scanlon MJ, Schembri MA, and Martin JL. DSB proteins and bacterial pathogenicity. *Nat Rev Microbiol* 7: 215–225, 2009.
26. Hogg PJ. Contribution of allosteric disulfide bonds to regulation of hemostasis. *J Thromb Haemost* 7(suppl 1): 13–16, 2009.
27. Hu SH, Peek JA, Rattigan E, Taylor RK, and Martin JL. Structure of TcpG, the DsbA protein folding catalyst from *Vibrio cholerae*. *J Mol Biol* 268: 137–146, 1997.
28. Inaba K. Disulfide bond formation system in *Escherichia coli*. *J Biochem* 146: 591–597, 2009.
29. Inaba K, Murakami S, Nakagawa A, Iida H, Kinjo M, Ito K, and Suzuki M. Dynamic nature of disulphide bond formation catalysts revealed by crystal structures of DsbB. *EMBO J* 28: 779–791, 2009.
30. Jakoby WB and Ziegler DM. The enzymes of detoxication. *J Biol Chem* 265: 20715–20718, 1990.
31. Jawad Z and Paoli M. Novel sequences propel familiar folds. *Structure* 10: 447–454, 2002.
32. Kadokura H, Katzen F, and Beckwith J. Protein disulfide bond formation in prokaryotes. *Annu Rev Biochem* 72: 111–135, 2003.
33. Kang JW, Jeong YJ, Kwon AR, Yun HJ, Kim DH, and Choi EC. Cloning, sequence analysis, and characterization of the astA gene encoding an arylsulfate sulfotransferase from *Citrobacter freundii*. *Arch Pharm Res* 24: 316–322, 2001.
34. Kang JW, Kwon AR, Kim DH, and Choi EC. Cloning and sequencing of the astA gene encoding arylsulfate sulfotransferase from *Salmonella typhimurium*. *Biol Pharm Bull* 24: 570–574, 2001.
35. Kim B, Hyun YJ, Lee KS, Kobashi K, and Kim DH. Cloning, expression and purification of arylsulfate sulfotransferase from *Eubacterium* A-44. *Biol Pharm Bull* 30: 11–14, 2007.
36. Kim DH, Hyun SH, Shim SB, and Kobashi K. The role of intestinal bacteria in the transformation of sodium picosulfate. *Jpn J Pharmacol* 59: 1–5, 1992.
37. Kim DH, Kim HS, Imamura L, and Kobashi K. Kinetic studies on a sulfotransferase from *Klebsiella* K-36, a rat intestinal bacterium. *Biol Pharm Bull* 17: 543–545, 1994.
38. Kim DH, Kim HS, and Kobashi K. Purification and characterization of novel sulfotransferase obtained from *Klebsiella* K-36, an intestinal bacterium of rat. *J Biochem* 112: 456–460, 1992.
39. Kim DH and Kobashi K. Kinetic studies on a novel sulfotransferase from *Eubacterium* A-44, a human intestinal bacterium. *J Biochem* 109: 45–48, 1991.
40. Kim DH and Kobashi K. The role of intestinal flora in metabolism of phenolic sulfate esters. *Biochem Pharmacol* 35: 3507–3510, 1986.
41. Kim DH, Konishi L, and Kobashi K. Purification, characterization and reaction mechanism of novel arylsulfotransferase obtained from an anaerobic bacterium of human intestine. *Biochim Biophys Acta* 872: 33–41, 1986.
42. Kim DH, Yoon HK, Koizumi M, and Kobashi K. Sulfation of phenolic antibiotics by sulfotransferase obtained from a human intestinal bacterium. *Chem Pharm Bull (Tokyo)* 40: 1056–1057, 1992.
43. Kobashi K, Fukaya Y, Kim DH, Akao T, and Takebe S. A novel type of aryl sulfotransferase obtained from an anaerobic bacterium of human intestine. *Arch Biochem Biophys* 245: 537–539, 1986.
44. Kobashi K, Kim D-H, Morikawa T. A novel type of arylsulfotransferase. *J Protein Chem* 6: 237–244, 1987.

45. Kwon AR, Oh TG, Kim DH, and Choi EC. Molecular cloning of the arylsulfate sulfotransferase gene and characterization of its product from *Enterobacter amnigenus* AR-37. *Protein Expr Purif* 17: 366–372, 1999.
46. Kwon AR, Yun HJ, and Choi EC. Kinetic mechanism and identification of the active site tyrosine residue in *Enterobacter amnigenus* arylsulfate sulfotransferase. *Biochem Biophys Res Commun* 285: 526–529, 2001.
47. Lasica AM and Jagusztyn-Krynicka EK. The role of Dsb proteins of gram-negative bacteria in the process of pathogenesis. *FEMS Microbiol Rev* 31: 626–636, 2007.
48. Lee NS, Kim BT, Kim DH, and Kobashi K. Purification and reaction mechanism of arylsulfate sulfotransferase from *Haemophilus* K-12, a mouse intestinal bacterium. *J Biochem* 118: 796–801, 1995.
49. Lide DR. *CRC Handbook of Chemistry and Physics*. Boca Raton, FL: Taylor & Francis Group, 2006/2007.
50. Lin D, Kim B, and Slauch JM. DsbL and DsbI contribute to periplasmic disulfide bond formation in *Salmonella enterica* serovar *Typhimurium*. *Microbiology (Reading, England)* 155: 4014–4024, 2009.
51. Lloyd AL, Rasko DA, and Mobley HL. Defining genomic islands and uropathogen-specific genes in uropathogenic *Escherichia coli*. *J Bacteriol* 189: 3532–3546, 2007.
52. Malojcic G. Structure and function of the wild-type transmembrane oxidoreductase DsbB and the arylsulfate sulfotransferase from uropathogenic *Escherichia coli*. PhD thesis: ETH Zurich, Zurich, Switzerland, 2008.
53. Malojcic G and Glockshuber R. Disulfide-bond formation and isomerization in prokaryotes. In: *RSC Biomolecular Sciences,* edited by Buchner J and Kiefhaber T. Weinheim: Royal Society of Chemistry, 2009, pp. 19–40.
54. Malojcic G, Owen RL, Grimshaw JP, Brozzo MS, Dreher-Teo H, and Glockshuber R. A structural and biochemical basis for PAPS-independent sulfuryl transfer by aryl sulfotransferase from uropathogenic *Escherichia coli*. *Proc Natl Acad Sci U S A* 105: 19217–19222, 2008.
55. Malojcic G, Owen RL, Grimshaw JP, and Glockshuber R. Preparation and structure of the charge-transfer intermediate of the transmembrane redox catalyst DsbB. *FEBS Lett* 582: 3301–3307, 2008.
56. Martin JL, Bardwell JC, and Kuriyan J. Crystal structure of the DsbA protein required for disulphide bond formation in vivo. *Nature* 365: 464–468, 1993.
57. Mathew JA, Tan YP, Srinivasa Rao PS, Lim TM, and Leung KY. *Edwardsiella tarda* mutants defective in siderophore production, motility, serum resistance and catalase activity. *Microbiol (Reading, England)* 147: 449–457, 2001.
58. Mobley HL, Green DM, Trifillis AL, Johnson DE, Chippendale GR, Lockatell CV, Jones BD, and Warren JW. Pyelonephritogenic *Escherichia coli* and killing of cultured human renal proximal tubular epithelial cells: role of hemolysin in some strains. *Infect Lmmun* 58: 1281–1289, 1990.
59. Mougous JD, Green RE, Williams SJ, Brenner SE, and Bertozzi CR. Sulfotransferases and sulfatases in mycobacteria. *Chem Biol* 9: 767–776, 2002.
60. Mougous JD, Petzold CJ, Senaratne RH, Lee DH, Akey DL, Lin FL, Munchel SE, Pratt MR, Riley LW, Leary JA, Berger JM, and Bertozzi CR. Identification, function and structure of the mycobacterial sulfotransferase that initiates sulfolipid-1 biosynthesis. *Nat Struct Mol Biol* 11: 721–729, 2004.
61. Paoli M. Protein folds propelled by diversity. *Prog Biophys Mol Biol* 76: 103–130, 2001.
62. Paxman JJ, Borg NA, Horne J, Thompson PE, Chin Y, Sharma P, Simpson JS, Wielens J, Piek S, Kahler CM, Sakellaris H, Pearce M, Bottomley SP, Rossjohn J, and Scanlon MJ. The structure of the bacterial oxidoreductase enzyme DsbA in complex with a peptide reveals a basis for substrate specificity in the catalytic cycle of DsbA enzymes. *J Biol Chem* 284: 17835–17845, 2009.
63. Pi N, Yu Y, Mougous JD, and Leary JA. Observation of a hybrid random ping-pong mechanism of catalysis for NodST: a mass spectrometry approach. *Protein Sci* 13: 903–912, 2004.
64. Raczko AM, Bujnicki JM, Pawlowski M, Godlewska R, Lewandowska M, and Jagusztyn-Krynicka EK. Characterization of new DsbB-like thiol-oxidoreductases of *Campylobacter jejuni* and *Helicobacter pylori* and classification of the DsbB family based on phylogenomic, structural and functional criteria. *Microbiology (Reading, England)* 151: 219–231, 2005.
65. Sambrook DW Jr. *Molecular Cloning: A Laboratory Manual*. New York: Cold Spring Harbor Press, 2001.
66. Schmidt B, Ho L, and Hogg PJ. Allosteric disulfide bonds. *Biochemistry* 45: 7429–7433, 2006.
67. Smith TF, Gaitatzes C, Saxena K, and Neer EJ. The WD repeat: a common architecture for diverse functions. *Trends Biochem Sci* 24: 181–185, 1999.
68. Teramoto T, Adachi R, Sakakibara Y, Liu MC, Suiko M, Kimura M, and Kakuta Y. On the similar spatial arrangement of active site residues in PAPS-dependent and phenolic sulfate-utilizing sulfotransferases. *FEBS Lett* 583: 3091–3094, 2009.
69. Teramoto T, Sakakibara Y, Liu MC, Suiko M, Kimura M, and Kakuta Y. Snapshot of a Michaelis complex in a sulfuryl transfer reaction: crystal structure of a mouse sulfotransferase, mSULT1D1, complexed with donor substrate and accepter substrate. *Biochem Biophys Res Commun* 383: 83–87, 2009.
70. Totsika M, Heras B, Wurpel DJ, and Schembri MA. Characterization of two homologous disulfide bond systems involved in virulence factor biogenesis in uropathogenic *Escherichia coli* CFT073. *J Bacteriol* 191: 3901–3908, 2009.
71. Vivian JP, Scoullar J, Robertson AL, Bottomley SP, Horne J, Chin Y, Wielens J, Thompson PE, Velkov T, Piek S, Byres E, Beddoe T, Wilce MC, Kahler CM, Rossjohn J, and Scanlon MJ. Structural and biochemical characterization of the oxidoreductase NmDsbA3 from *Neisseria meningitidis*. *J Biol Chem* 283: 32452–32461, 2008.
72. Voet D and Voet JG. *Biochemistry*. New York: John Wiley and Sons, 2004.
73. Welch RA, Burland V, Plunkett G 3rd, Redford P, Roesch P, Rasko D, Buckles EL, Liou SR, Boutin A, Hackett J, Stroud D, Mayhew GF, Rose DJ, Zhou S, Schwartz DC, Perna NT, Mobley HL, Donnenberg MS, and Blattner FR. Extensive mosaic structure revealed by the complete genome sequence of uropathogenic *Escherichia coli*. *Proc Natl Acad Sci U S A* 99: 17020–17024, 2002.
74. Wouters MA, George RA, and Haworth NL. "Forbidden" disulfides: their role as redox switches. *Curr Protein Peptide Sci* 8: 484–495, 2007.
75. Wouters MA, Lau KK, and Hogg PJ. Cross-strand disulphides in cell entry proteins: poised to act. *Bioessays* 26: 73–79, 2004.

76. Wunderlich M and Glockshuber R. Redox properties of protein disulfide isomerase (DsbA) from *Escherichia coli*. *Protein Sci* 2: 717–726, 1993.
77. Zhou Y, Cierpicki T, Jimenez RH, Lukasik SM, Ellena JF, Cafiso DS, Kadokura H, Beckwith J, and Bushweller JH. NMR solution structure of the integral membrane enzyme DsbB: functional insights into DsbB-catalyzed disulfide bond formation. *Mol Cell* 31: 896–908, 2008.

Abbreviations Used

ASST = aryl sulfotransferase
Dsb = disulfide bond
MUS = 4-methylumbelliferylsulfate
PAPS = 3′-phosphate-5′-phosphosulfate
PNS = *p*-nitrophenylsulfate
RNA = ribonucleic acid

Address correspondence to:
Dr. Goran Malojčić
Institute of Molecular Biology and Biophysics
ETH Zurich
CH-8093 Zurich
Switzerland

E-mail: goran@mol.biol.ethz.ch

Date of first submission to ARS Central, January 28, 2010; date of final revised submission, February 6, 2010; date of acceptance, February 6, 2010.